www.vbripress.com, www.amlett.com, DOI: 10.5185/amlett.2010.10171 Published online by the VBRI press in 2011

Optical properties of $MAl_{12}O_{19}$:Eu (M = Ca, Ba, Sr) nanophosphors

Abhay D. Deshmukh[1], S. J. Dhoble[1]*, N.S. Dhoble[2]

[1]*Department of Physics, RTM Nagpur University, Nagpur 440033, India*

[2]*Department of Chemistry, Sevadal Mahila Mahavidhyalaya, Nagpur 440009, India*

*Corresponding author. Tel: (+91) 712 2500083; Fax: (+91) 712 2532841; E-mail: sjdhoble@rediffmail.com

Received: 3 Oct 2010, Revised: 20 Nov 2010 and Accepted: 23 Nov 2010

ABSTRACT

The $MAl_{12}O_{19}$:Eu (M = Ca, Ba, Sr) phosphor were synthesized by combustion method and systematically characterized by photoluminescence excitation and emission spectra, concentration quenching, morphology and X-ray mapping with scanning electron microscopy. In $SrAl_{12}O_{19}$:Eu phosphor two PL emission peaks are observed at about 389 nm and another around 420 nm as well as $BaAl_{12}O_{19}$:Eu phosphor shows blue emission around 460 nm is observed in the blue region of the spectrum and $CaAl_{12}O_{19}$:Eu shows only red emission at 592 as well as 615nm. Both phosphors can be efficiently excited in the wavelength range of 250-425 nm, where the near UV (~320 nm) solid state excitation is matched. By combining $MAl_{12}O_{19}$:Eu (M = Ca, Ba, Sr) phosphor with near UV chops emitting intense blue green (Ba), yellow-red (Ca) and blue purple (Sr) LEDs white LEDs can be produced.

Keywords: Phosphor; photoluminescence; SEM; X-ray diffraction, nanophosphors; LEDs.

Abhay D. Deshmukh did his M.Sc. in 2006 from Nagpur University, India. At present, he is a doctoral candidate at Nagpur University, registered in NEERI (National Environmental Engineering Research Institute); CSIR Laboratory. His doctoral work is titled 'Development of Microcrystalline and Nanostructured Aluminate Luminescent Materials'. This study investigates the development of new materials which satisfies the requirements of phosphor used in lighting luminaries. He is currently working as Research Associate at the National Physical Laboratory, New Delhi, India. The aim of this work is to develop the materials which convert the visible light to UV light. He has also worked as Project Associate at Department of MME, IIT Madras, India on improvement of notch rupture life of 718 super alloys.

S.J. Dhoble obtained M.Sc. degree in Physics from Rani Durgavati University, Jabalpur, India in 1988. He obtained his Ph.D. degree in 1992 on Solid State Physics. Dr. Dhoble is presently working as an associate professor in Department of Physics, R.T.M. Nagpur University, Nagpur, India. During his research carrier, he is involved in the synthesis and characterization of solid state lighting nanomaterials as well as development of radiation dosimetry phosphors using thermoluminescence, mechanoluminescence and lyoluminescence techniques. He is an executive member of Luminescence Society of India.

N.S. Dhoble obtained M.Sc. degree in Chemistry from Nagpur University, Nagpur, India in 1988. She did Ph.D. in 1993 on Radiation Chemistry. Dr. Dhoble is presently working as an associate professor in Department of Chemistry, Sevadal Mahila Mahavidhyalaya, Nagpur, India. During her research carrier, she is involved in the synthesis and characterization of nanomaterials for lamp and radiation dosimetry. She is a member of Luminescence Society of India.

Introduction

Rare-earth and non-rare-earth-doped inorganic phosphors are widely used in a variety of applications, such as lamp industry, radiation dosimetry, X-ray imaging, and colour display. In particular, the luminescent properties of europium-ion doped phosphors have been studied extensively for their applications in these areas [**1, 2**]. Eu^{2+} activated phosphors MAl_2O_4 and $MAl_{12}O_{19}$ (M = Sr, Ba, Ca, Mg) are well known since the studies by Blasse and Brill [**3**] in the 1960s. Their researches lead to the conclusion that these compounds were adequate phosphorescent materials because of their high quantum efficiency in the visible region. The emission of Eu^{2+} ions varies from blue to red depending on the host lattice due to crystal-field effects [**2**]. A completely new generation of persistent luminescent phosphors, Eu^{2+} doped alkaline earth

aluminates, $MAl_2O_4:Eu^{2+}$ (M = Ca, Sr), has been developed to replace ZnS:Cu [**4**]. At present, complex aluminates [**5**] as well as other materials [**6**] are subject to investigation.

Up to date, very little literatures reported the synthesis of nanostructured $MAl_{12}O_{19}$ (M = Ca, Ba, Sr) by combustion method. Douy and Capron [**7**] prepared $SrAl_{12}O_{19}$ powders by spray-drying aqueous solutions of strontium and aluminium nitrates followed by heating the powders to decompose the nitrates. Chen et al. [**8**] synthesized Eu^{2+} and Dy^{3+} co-doped $SrAl_{12}O_{19}$ by a sol–gel process. In fact, $BaAl_{12}O_{19}$:Mn is known as a green-emitting phosphor for PDPs [**9**], and Pr- or Nd-doped $SrAl_{12}O_{19}$ crystals has been suggested as one of the potential material with good laser properties [**10**]. In this article, we reported the synthesis of nanostructured $MAl_{12}O_{19}$:Eu (M = Ca, Ba, Sr) phosphors via combustion root synthesis, using urea as fuel and the effect of the Ca Ba and Sr in $MAl_{12}O_{19}$ on PL properties was investigated.

Experimental

The $(Ca,Ba,Sr)_{1-x}Al_{12}O_{19}:Eu_x$ (x = 1%, 3% and 5%) phosphor doped with Eu ions were prepared through a low temperature initiated combustion process. The starting material were taken as aluminium nitrate $[Al(NO_3)_3.9H_2O]$, Calcium nitrate $[Ca(NO_3)_2.6H_2O]$. Europium nitrate was prepared by dissolving europium oxide $[Eu_2O_3]$ in nitric acid. All the reagents were of analytical grade from Merck with 99.99% purity were used without further purification. The correct amount of each excess urea $[CO(NH_2)_2]$ were injected into the precursor solution or these compositions. The amount of metal nitrates (oxidizers) and urea (fuel) were calculated using the total oxidizing and reducing valencies of the components, which serve as the numerical coefficients so that the equivalence ratio is unity and the heat liberated during combustion is at a maximum. After stirring for about 15 min, precursor solution was transferred to a furnace preheated to 400°C and 500°C, the porous products were obtained.

The phase composition and phase structure were characterized by X-ray diffraction (XRD) pattern using a PAN-analytical diffractometer with Cu Kα radiation (λ = 1.5405 A^0) operating at 45kV, 40mA. The morphology and the composition of the products were examined by scanning electron microscopy (SEM, JED-2300) equipped with an energy-dispersive spectrometry (EDS). Energy dispersive spectrometry (EDS) attached to the JEOL 2300 was used to determine the composition of the products. The photoluminescence properties of the phosphor (excitation and emission) were measured using a Shimadzu RF5301PC Spectroflurophotometer at room temperature.

Results and discussion

Structural property

The overall structure and phase purity of as synthesized products were characterized by XRD. **Fig. 1** shows a typical XRD pattern of the $M_{1-x}Al_{12}O_{19}:Eu_x$ (M = Ca, Ba, Sr). All the phosphors are hexagonal structure with the space group P63/mmc. The diffraction peaks of $BaAl_{12}O_{19}$, $SrAl_{12}O_{19}$ and $CaAl_{12}O_{19}$ can be easily indexed with the JCPDS card no 00-026-0135, card no. 00-026-0976 and card no. 00-25-0122 respectively. No other crystalline phases were detected within the detection limit. The XRD results indicated that the as synthesized products are highly pure, single-phase.

The small amount of doped rare earth ions has virtually no effect on the phase structures. The average sizes calculated from XRD reflections for $BaAl_{12}O_{19}$, $CaAl_{12}O_{19}$ and $SrAl_{12}O_{19}$ by application of Scherrer's equation are 40, 51 and 51 nm, respectively. It is known that the full-width at half-maximum (FWHM) can be expressed as a linear combination of the contribution from the lattice strain and crystalline size. The effects of the strain and particle size on the FWHM can be expressed by the following equation:

$$D_{hkl} = 0.9\,\lambda / \beta \cos\theta$$

where β is the measured FWHM (in radians), θ is the Bragg angle of the peak, λ is the X-ray diffraction wavelength.

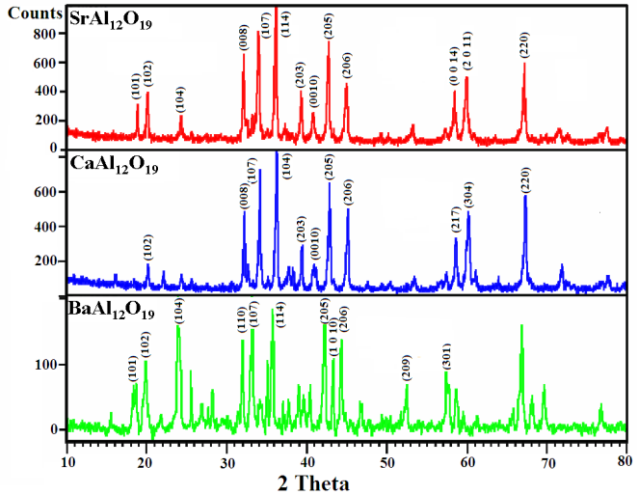

Fig. 1. XRD pattern of $SrAl_{12}O_{19}$, $CaAl_{12}O_{19}$ and $BaAl_{12}O_{19}$.

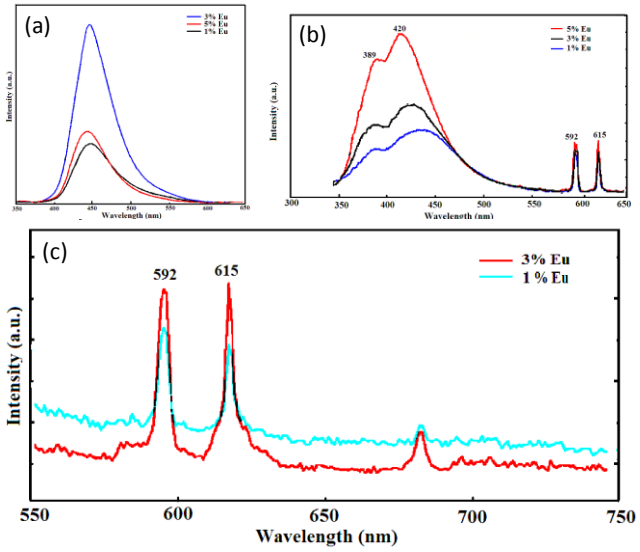

Fig. 2. Photoluminescence of (a) $BaAl_{12}O_{19}$: Eu, (b) $SrAl_{12}O_{19}$: Eu and (c) $CaAl_{12}O_{19}$: Eu.

Photoluminescence properties

Europium ions can be stabilized in host lattice in either divalent or trivalent oxidation state. The incorporation and stabilization of Eu ions in the sample were confirmed by the luminescence investigations. The photoluminescence emission spectra for the $M_{1-x}Al_{12}O_{19}$: Eu_x (M = Sr, Ba, Ca) phosphors by 320 nm excitation shown in **Fig. 2 a-c**. The spectra consist of broad, single peaked emission band in the blue region of the spectrum in $M_{1-x}Al_{12}O_{19}$: Eu_x (M = Ba, Sr) phosphors. These bands were assigned to the Eu^{2+} ions ($4f^7 \rightarrow 4f^6 5d^1$ transition), judging from the range of wavelength. The peak position slightly shifted higher wavelength with the increase of Eu^{2+} ions. Two emission peaks were recognized at 389 and 420 nm for $Sr_{1-x}Eu_xAl_{12}O_{19}$ and at 460 nm for $Ba_{1-x}Eu_xAl_{12}O_{19}$. The ratio of two peaks almost fixed, although the intensity of two peaks varied with x. The intensity with different concentration of Eu^{2+} ions shows a specific pattern. The intensity reached a maximum at x = 0.05 for $Sr_{1-x}Eu_xAl_{12}O_{19}$ and x = 0.03 for $Ba_{1-x}Eu_xAl_{12}O_{19}$. The PL emission in $Ca_{1-x}Eu_xAl_{12}O_{19}$ phosphor observed at 592 and 615 nm sharp peaks in the red region of the spectrum due to $^5D_0 \rightarrow {}^2F_0$ and $^5D_0 \rightarrow {}^2F_1$ transition of Eu^{3+} ion, in this phosphor Eu^{3+} ion may be enter in side symmetry of lattice of the host material during preparation of phosphor as well changing matrix crystal structure and formation of aggregation of nanopartilces, therefore Eu ion observed in the Eu^{3+} valance state. The intensity with different concentration of Eu^{3+} ions shows a specific pattern. The intensity reached a maximum at x = 0.03 for $Ca_{1-x}Eu_xAl_{12}O_{19}$.

Fig. 2a, **b** and **c** show the emission spectrum of $BaAl_{12}O_{19}$:Eu^{2+}, $SrAl_{12}O_{19}$:Eu^{2+} and $CaAl_{12}O_{19}$: Eu^{3+} at the 320 nm excitation. At this excitation it is observer that the Eu ions are incorporated in divalent form in $BaAl_{12}O_{19}$:Eu^{2+} and $SrAl_{12}O_{19}$:Eu^{2+} phosphors. Arakawa [11] reported the emission of $SrAl_{12}O_{19}$:Eu for 325 nm excitation prepared by solid state reaction at 390, 480 and 530 nm for $BaAl_{12}O_{19}$:Eu phosphor. In present study, the combustion method is applied to prepare the phosphor. Due to rapid and high temperature, the nano crystalline size particles are formed. In our case the main peaks of emission spectra of the luminescent nanoparticles shift to shorter wavelength (from 590 to 460 nm and then to 420 nm) in $BaAl_{12}O_{19}$: Eu^{2+} and $SrAl_{12}O_{19}$: Eu^{2+} correspondingly, the luminescence changes from yellow-red to blue-green and then to blue-purple. This phenomenon is derived from the changing matrix crystal structure. The Sr^{2+}/ Ba^{2+} and Eu^{2+} ions are very similar in their ionic size (i.e. 1.12 A˚/1.35 A˚ and 1.20 A˚, respectively). Consequently, when occupied by Eu^{2+} ions, the Sr^{2+}/Ba^{2+} sites will have quite similar local distortions and the influence on the $SrAl_{12}O_{19}$/ $BaAl_{12}O_{19}$ crystal structure is small. But the radii of Ca^{2+} (i.e. 0.99) is different from Eu^{2+}. So, the structure of $CaAl_{12}O_{19}$ will be greatly distorted when the Ca^{2+} sites are occupied by Eu^{3+} ions. Anamorphic crystal lattices result when the surroundings of Eu^{3+} are changed and so the emission wavelengths change correspondingly. When Eu^{3+} substitutes for Ca^{2+} in $CaAl_{12}O_{19}$:Eu^{3+} experiences lesser repulsion owing to the expansion of the crystal lattice. In contrast, when Eu^{2+} substitutes for Sr^{2+}/ Ba^{2+} in $SrAl_{12}O_{19}$/ $BaAl_{12}O_{19}$, Eu^{2+} endures lesser attraction owing to shrinkage of the crystal lattice. This is why the wavelength

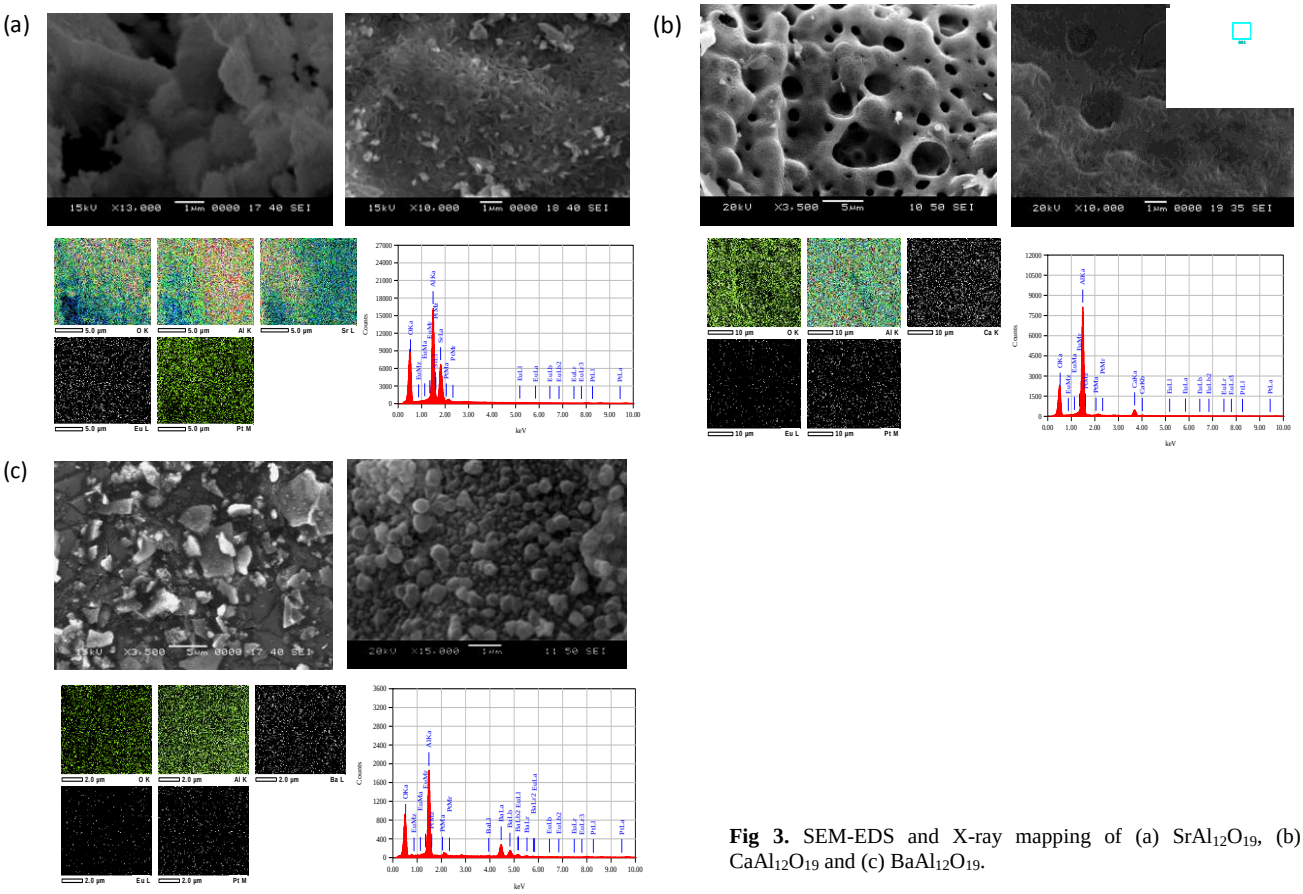

Fig 3. SEM-EDS and X-ray mapping of (a) $SrAl_{12}O_{19}$, (b) $CaAl_{12}O_{19}$ and (c) $BaAl_{12}O_{19}$.

of $CaAl_{12}O_{19}$: Eu^{3+}, shifts to a longer wavelength compared with $BaAl_{12}O_{19}$: Eu^{2+}. $M_{1-x}Eu_xAl_{12}O_{19}$ (M = Sr, Ba) has a magnetoplumbite structure and is β-alumina type material. It is well known that there are four possible occupying positions for optically active ions in β-alumina. That is, these positions are Beevers-Ross (BR) and mid-oxygen (mO) sites in the conduction plane, and four-fold Al(2), (3) and six-fold Al(1) and (4) within the spinel block. The position of these alkaline earth ions in the conduction plane of β-alumina is generally determined by short-range Coulomb interaction according to ionic radius. Accordingly, Ba^{2+} ions are only located at the BR site by Coulomb interaction due to large ionic radius, whereas Sr ions can be located at both BR and mO sites due to intermediate ionic radius. Therefore the emission spectra with two peaks for $Sr_{1-x}Eu_xAl_{12}O_{19}$ can be easily understood. It is also seen form the SEM images and X-ray mapping that the Eu^{2+} ions are not entering into the lattice but replace the Ba and Sr ions in, $BaAl_{12}O_{19}$: Eu^{2+} and $SrAl_{12}O_{19}$: Eu^{2+} lattice easily and side symmetry in $CaAl_{12}O_{19}$: Eu^{3+} phosphor due to Eu^{3+} ion .

Morphology and X-ray mapping

The typical morphology and X-ray mapping of powders is shown in **Fig. 3**, which displays an SEM micrograph of a powder synthesized by combustion method. **Fig. 3a** shows the $SrAl_{12}O_{19}$: Eu powder, which is formed by large porous aggregates, with typical sizes of 1–10 μm (**Fig. 3a**). In **Fig. 3b**, micrographs of $CaAl_{11}O_{12}$: Eu shows the pores produced by the fast expulsion of gases during the combustion process can be observed. SEM observations with higher magnification showed that these aggregates were constituted by nanoparticles. It is worth remarking that the shape of nanoparticles is typical of powders synthesized by the combustion process, and it has been found for other materials [**12, 13**]. This is an important result, since it confirms that the calcination temperature can be reduced in order to get a higher specific surface area and a smaller crystallite size. Moreover, in some faces the holes are observed which formed during the gas evolution such as N_2, H_2 and nascent oxygen. **Fig. 3a** show the $SrAl_{12}O_{19}$: Eu phosphor consists of a flower like structure, while more porous and dense nano rod like structure is observed at higher magnification for $CaAl_{12}O_{19}$: Eu (**Fig. 3b**). In contrast, the $BaAl_{12}O_{19}$: Eu (**Fig. 3c**) show phosphor which comprises of nano size spherical particles.

Conclusion

In present work $M_{1-x}Al_{12}O_{19}$: Eu_x (M = Ca, Ba, Sr) phosphor were synthesized by combustion method and their optical properties investigated. The main peaks of emission spectra of the luminescent nanoparticles shift to shorter wavelength (from 590 to 460 nm and then to 420 nm) in $BaAl_{12}O_{19}$: Eu^{2+} and $SrAl_{12}O_{19}$: Eu^{2+} phosphors correspondingly, the luminescence changes from yellow-red to blue-green and then to blue-purple and Eu^{3+} emission in red region observed in $CaAl_{12}O_{19}$: Eu^{3+} phosphor due to aggregation of nanopartilces. By combining $MAl_{12}O_{19}$: Eu (M = Ca,Ba,Sr) phosphor with near UV chops, intense blue green (Ba), blue purple (Sr) and yellow-red (Ca)

LEDs, white LED can be produced. The emission spectra for 320 nm excitation (Solid state excitation) are 3 times superior to 254 nm excitation (Mercury excitation). These results shows that the $MAl_{12}O_{19}$: Eu (M = Ca, Ba, Sr) phosphor exhibit potential application in the field of white LEDs.

References

1. Shionoya, S.; Yen, W.M., *in Phosphor Hand Book*, CRC Press, Washington DC, **1999**, 391–432.
2. Poort, S.H.; Blokpoel, W.P.; Blasse, G. *Chem. Mater.* **1995**,*7*,1547 **DOI:** 10.1021/cm00056a022
3. Blasse, G.; Brill, A. *Philips Res. Rep.* **1968**, *23*, 201.
4. Murayama, Y.; Takeuchi, N.; Aoki, Y.; Matsuzawa, T. US Patent 5,424,006, **1995**.
5. Nakamura, T.; Kaiya, K.; Takahashi, N.; Matsuzawa, T.; Rowlands, C.C.; Beltran-Lopez, V.; Smith, G.M.; Riedi, P.C. *J. Mater. Chem.* **2000**, *10*, 2566. **DOI:** 10.1039/B004061O
6. Qiu, J.; Gaeta, A.L.; Hirao, K. *Chem. Phys. Lett.* **2001**, *333*, 236. **DOI:** 10.1016/S0009-2614(00)01362-2
7. Douy, A.; Capron, M. *J. Eur. Ceram. Soc.* **2003**, 23, 2075. **DOI:** 10.1016/S0955-2219(03)00015-3
8. Chen, I.C.; Chen, T.M. *J. Mater. Res.* **2001**, *16*, 1293. **DOI:** 10.1557/JMR.2001.0181
9. Lee, D.Y.; Kang, Y.C.; Park, H.D.; Ryu, S.K. *J. Alloys Compounds* **2003**, *353*, 252. **DOI:** 10.1016/S0925-8388(02)01197-0
10. Merkle, L.D.; Zandi, B.; Moncorge, R.; Guyot, Y.; Verdun, H.R.; McIntosh, B. *J. Appl. Phys.* **1996**, *79*, 1849. **DOI:**10.1063/1.361085
11. Arakawa, T.; Nagata, N. J. *Alloys and Compounds* **2006**, *408*, 864. **DOI:** 10.1016/j.jallcom.2005.01.074
12. Fraigi, L.B.; Lamas, D.G.; Walso¨e de Reca, N.E. *Mater. Lett.* **2001**, *47*, 262. **DOI:** 10.1016/S0167-577X(00)00246-9
13. Bianchetti, M.F.; Jua´rez , R.E.; Lamas, D.G.;Walso¨e de Reca, N.E.; Pe´rez, L.; Cabanillas, E. *J. Mater. Res.* **2002**, *17*, 2185. **DOI:** 10.1557/JMR.2002.0169

